ELSEVIER

Journal of Structural Geology 27 (2005) 265–281

JOURNAL OF STRUCTURAL GEOLOGY

www.elsevier.com/locate/jsg

Effect of water on the strength and microstructure of Carrara marble axially compressed at high temperature

J.H.P. De Bresser[a,*], J.L. Urai[b], D.L. Olgaard[c]

[a]*HPT-laboratory, Department of Earth Sciences, PO Box 80.021, 3508 TA Utrecht University, the Netherlands*
[b]*Geologie-Endogene Dynamik, RWTH, Aachen, Germany*
[c]*ExxonMobil Upstream Research Company, Houston, Texas, USA*

Received 18 November 2003; received in revised form 25 August 2004; accepted 12 October 2004
Available online 7 January 2005

Abstract

In this study, we aimed to (i) answer the question if water affects the strength of marble deforming at high temperature and (ii) establish criteria that allow assessment of the role of water in microstructure development in marble. Samples of Carrara marble were axially compressed at temperatures ranging 600–1000 °C and strain rate $\sim 10^{-5}$ s^{-1}, with or without addition of 0.4–2.1 wt% water. Water-added samples were found to be slightly weaker than dry samples. Microstructurally, all samples showed grain flattening and twinning at 600 °C and dynamic recrystallization dominated by grain boundary migration at higher temperature. Grain boundaries in wet samples showed isolated or semi-continuous remnants of fluid pockets. The average grain roundness R and fractal dimension D relating grain diameter d and grain perimeter P ($P \propto d^D$) for wet recrystallized samples were systematically lower than for dry samples. At 600 °C, high pore fluid pressure probably enhanced dilatation of wet samples and helped grain boundary sliding (GBS), thereby lowering the strength. At higher temperature, fluid-enhanced grain boundary migration served as a recovery process, reducing the contribution of GBS to creep. Overall, water has little effect on strength and microstructure of marble experimentally deformed at high temperature.

Keywords: Calcite; Water; Microstructure; Recrystallization; Weakening

1. Introduction

It is well established that water causes rheological weakening of Earth materials (Carter et al., 1990; De Meer et al., 2002). Water can cause hydraulic fracturing, enhance diffusion along grain boundaries and affect intracrystalline dislocation processes ('hydrolytic weakening'). Further, water may have an indirect influence on the mechanical behavior of rocks by assisting metamorphic reactions that produce a new mineral assemblage with a strength that is different from that of the original aggregate (e.g. Rubie, 1990; Rutter and Brodie, 1995). The influence of water on rock deformation is important at all lithospheric conditions, from the brittle behavior of the upper crust to ductile flow at a deeper level.

A large body of experimental data already exists on the effect of water during high temperature (ductile) deformation of Earth materials. Water weakening during ductile flow has been observed experimentally in quartz (e.g. Kronenberg et al., 1986; Post et al., 1996), feldspar (e.g. Rybacki and Dresen, 2000), olivine (e.g. Karato et al., 1986; McDonnell et al., 1999; Mei and Kohlstedt, 2000a,b) and rock salt (e.g. Urai et al., 1986b; Watanabe and Peach, 2002). Mechanisms proposed to explain this weakening include (a) water fugacity controlling the concentration of point defects and thereby affecting solid state grain boundary diffusion (Tullis and Yund, 1991; Mei and Kohlstedt, 2000a) or solid state lattice diffusion and dislocation climb (Post et al., 1996; Mei and Kohlstedt, 2000b), (b) water creating thin aqueous grain boundary films that facilitate pressure solution (Spiers and Carter, 1998), (c) water promoting the development of interconnected weak layers of melt along grain boundaries (Van der Molen and Paterson, 1979; Hirth and Kohlstedt, 1995), (d)

* Corresponding author. Tel.: +31-30-253-4973; fax: +31-30-253-7725
E-mail address: j.h.p.debresser@geo.uu.nl (J.H.P. De Bresser).

0191-8141/$ - see front matter © 2005 Elsevier Ltd. All rights reserved.
doi:10.1016/j.jsg.2004.10.002

water inducing a transition from strong to weak type of crystallographic preferred orientation (Jung and Karato, 2001), and (e) water assisting dynamic recrystallization by enhancing grain boundary migration rates, allowing recrystallization to act as a recovery mechanism (Urai et al., 1986a; Peach et al., 2001). Studies on naturally deformed rocks have confirmed that the experimental results are relevant for our understanding of the role of localized deformation zones in the tectonic evolution of the lithosphere (e.g. Kronenberg et al., 1990; Hirth and Kohlstedt, 1996).

One important rock-forming mineral not yet mentioned above is calcite. Calcite tectonites play an important role in many crustal deformation zones and numerous experiments have been performed on calcite materials to constrain its strength. A wide range of materials and experimental conditions have been explored (see Renner et al., 2002b), but only limited attention has been paid to the role of water in calcite deformation. Recent compaction experiments by Dewers and Muhuri (2000) and Zhang et al. (2002) on wet granular calcite showed intergranular pressure solution at low temperature and low applied stress, with or without cataclastic deformation. Pressure solution is important in carbonate diagenesis and fault sealing at shallow depths. For deformation at deeper crustal levels, De Bresser et al. (2002) compared strengths of naturally deformed calcite rocks as predicted by flow laws with estimates based on microstructural (piezometric) constraints, revealing some puzzling inconsistencies. Part of the discrepancy may arise from our limited understanding of the role of water in deformation of dense calcite rock. The early work of Adams and Nicolson (1900) comprised one deformation test on wet Carrara marble at $T=300$ °C that could be compared with a dry-deformed counterpart. No influence of water was observed. Griggs et al. (1951, 1953) performed experiments on Yule marble with interstitial water at $T=150$ and 300 °C. They noted mechanical weakening due to the pressure exerted by the water, but found no evidence for any appreciable effect on flow or recrystallization of the marble under the imposed conditions. Heard (1960) described the results of some experiments at 150 °C on Solnhofen limestone with pore fluid, and this work was later extended by Rutter (1972, 1974) who systematically tested the strength of Carrara marble and Solnhofen limestone with and without pore water at T ranging from 20 up to 500 °C. Rutter found that water weakens fine-grained limestone as long as the temperature is relatively low, in line with the results of Heard (1960), but has little effect on the rheological behavior of course-grained marble. Finally, Olgaard (1985) carried out a few experiments on synthetic calcite rock (grain size ~10–20 μm) at $T=700$ °C and found little difference in strength between wet and dry calcite rock.

In the present study, we aimed to investigate the role of water on the deformation of calcite marble at high temperature ($T\geqq 600$ °C), at conditions not covered before with wet material. We particularly concentrated on the effect of water on microstructural modification compared with its effect on mechanical behavior, since microstructures form the link between experimental results and natural deformation structures. In this way, we obtained criteria that help interpret natural (calcite) rocks in terms of the influence of water on their deformation.

2. Samples and experimental method

Cylindrical samples of marble were cored from a block of white 'Bianco Ordinario' from a quarry near Carrara, Italy. The marble has a connected porosity of ~0.1%. Trace element content of this marble is given in Table 1, together with measurements from Carrara marble samples used in other experimental studies. The tested samples were 10 mm in diameter and ~20 mm in length, and were jacketed in Pt capsules. One set of samples was dried in an oven at 300 °C prior to jacketing. Distilled water was added to the other samples, in amounts corresponding to 0.4–2.1 wt%. The Pt jackets were immediately sealed after the water was added, by welding while frozen in liquid N_2. The sealed capsules were carefully weighed to check for loss of water during sealing. After the deformation experiment, a small hole was punched into the Pt jacket and weight loss over time was monitored, to confirm that the samples did not dry-out during deformation.

The sealed Pt capsules were mounted into an assembly with zirconia pistons (with alumina end pieces between Pt capsule and piston) inside an iron jacket that was oxidized to prevent the iron and platinum jackets from sticking to each other. An S-type thermocouple was mounted in the central bore of one of the pistons, allowing temperature measurement within a few millimeters of one end of the sample capsule. The complete piston-sample assembly was inserted into an argon gas-medium testing machine at ANU, Canberra, Australia (Paterson, 1990). This machine consists of a loading frame holding an internally heated pressure vessel with an internal load cell. In the set-up used, the thermal gradient along the samples was less than 5 °C. Deformation experiments were carried out at temperatures in the range $T=600$–1000 °C, confining pressure 300 MPa, and strain rate $\dot{\varepsilon}\sim 1\times 10^{-5}$ s^{-1}, with one test at 1×10^{-4} s^{-1}. Maximum axial strains (ε) achieved were 20%. At the end of the test, the furnace was switched off and the deformation piston was retracted. The system was depressurized when $T\leq 400$ °C, which lowered the risk of post-experiment dilatation. The raw load–displacement data were processed to obtain true stress–strain curves by assuming homogeneous deformation at constant volume, and correcting for apparatus distortion and strength of the iron jacket. Separate deformation tests were carried out on iron tubes to calibrate the strength of the jackets. Taking all uncertainties into account, the error in measured stress was estimated to be ~5%.

In addition to the deformation experiments, two heat

Table 1
Trace element chemistry of Carrara marble, analyzed by Inductively Coupled Plasma (ICP) Emission Spectrophotometry. Values are in ppm. The samples used in the present study were cored from block 'carr1' (measurements a and b) and 'carr4'. The trace element chemistry can be compared with measurements from Carrara marble used in other studies (carr-tH from Ter Heege et al. (2002) and carr_dB from De Bresser (2002)). Note that this method does not distinguish between impurities in solid solutions and in second phases

Element	Carr 1a	Carr 1b	Carr 4	Carr_dB	Carr_tH
Sr	135.0	135.0	120.0	133.1	97.0
Ce	62.0	61.0	61.0	77.8	7.0
Co	0.3	0.5	0.3		
Be	0.1	0.1	0.1	0.1	0.2
Ba	3.0	1.8	1.4		
B	3.3	1.4	1.0		
Mn	11.0	10.0	10.0	25.2	27.0
Fe	150.0	93.0	24.0		12.0
P	22.0	14.0	13.0	25.0	6.0
S	1440.0	1454.0	1430.0		
Mg	4804.0	5845.0	3391.0	3221.0	2250.0
Si	105.0	49.0	55.0		
V	5.9	5.3	5.1	6.5	0.8
Na	108.0	122.0	90.0		
Al	80.0	20.0	28.0		
Zn	33.0	27.0	25.0	0.5	1.0
Cu	5.2	4.6	4.3	4.0	1.0
Li	0.1	0.3	0.2		
Ni	0.0	0.0	0.9		
Ti	5.1	4.0	4.0	7.9	24.0
Y	2.3	1.9	1.2	1.8	1.3
K	19.0	0.0	12.0		4.0
Cr	3.3	2.6	2.6	2.6	27.0

treatment tests were performed at 800 °C, using one pre-dried and one water-added sample. The duration of the heat treatment was similar to the duration of the deformation tests at 800 °C.

After the experiments, the samples were cut lengthways and double-polished ultra-thin sections (thickness 5–10 μm) were prepared. Microstructural study of the thin sections was carried out using a Leica DMRX light optical polarization microscope. Further, a Cambridge S360 scanning electron microscope (SEM) was used to study grain boundaries in split samples. Quantitative analysis of microstructures in thin sections was done using on-screen manual tracings of stacked digital images of different polarization contrast (e.g. Heilbronner and Tullis, 2002). For all samples, only the central part of the sample was studied, using one magnification (5× objective, covering ~3 mm^2 of sample area) to avoid scale-dependent bias in the data acquisition. The traced micrographs were analyzed using the image analysis program Leica QWin Pro (version 2.2) for quantification of grain area (A), perimeter (P), roundness (R) and aspect ratio. Grain areas were used to calculate equivalent circular diameters (d) as representation of the grain size. No stereological correction for sectioning effects was applied. Grain roundness R is calculated by QWin using:

$$R = \frac{P^2}{1.064(4\pi A)} \quad (1)$$

The adjustment factor of 1.064 in Eq. (1) corrects the perimeter for corner effects produced by digitization of the grain microstructure. Smaller values of roundness indicate grain shapes that approach ideal circles. For the grain aspect ratio, the *Feret*90/*Feret*0 ratio of the width and height of the grains measured perpendicular and parallel, respectively, to sample long axis (i.e. load direction) was used. This ratio can be compared directly with the strain ratio resulting from the imposed amount of deformation. We quantified this comparison of Feret and strain ratio by:

$$F_s = \frac{Feret90/Feret0}{(s_1/s_3)(Feret90/Feret0)_{start}} \quad (2)$$

where s_1/s_3 is the strain ratio of ideal spherical grains deformed to the bulk strain of the given experiment (i.e. the ratio of maximum and minimum stretch assuming constant volume) and $(Feret90/Feret0)_{start}$ is the Feret ratio of the undeformed starting material, for which $s_1/s_3 = 1$. Values for F_s near to unity imply grain aspect ratio's that closely track the imposed strain. Note that in axisymmetric deformation, as applied here, the 'intermediate' stretch s_2 is not 1 (i.e. deformation is not plane strain) but equals s_1. As a consequence, axisymmetric compression results in a small apparent grain size reduction in 2D sections due to movement of material out of the plane of section, in the order of 5% for an axial compression of 10%. However, this does not influence calculation of F_s as long as the correct value for s_1 is used.

3. Mechanical data

The results of the experiments on wet and dry Carrara marble are given in Table 2. All stress–strain curves (Fig. 1) show a sharp yield-point at 1–2% shortening, followed by smooth stress–strain behavior. At 600 °C, the samples showed continuous work hardening up to strains of at least 18%. At higher temperature, the behavior after yield was quasi-steady state or exhibited limited strain weakening. With one exception at 800 °C, the strength of wet samples was slightly but significantly lower than that of pre-dried samples (Figs. 1 and 2). At 600 °C, the strength of the wet sample, at 5% strain (Table 2), was almost 40% lower than that of the dry sample. At 900–1000 °C, the difference in strength between wet and dry marble decreased to about 10%. These differences in strength were outside the experimental uncertainty. Note, however, that at 800 °C substantial differences in strength were observed between experiments performed at identical conditions.

The stress measured in one test with strain rate 10 times faster than applied in all other tests (#5359, $T=1000$ °C—see Table 2) was used to assess the strain rate sensitivity of flow stress. Taking a conventional power law relation between strain rate and flow stress of the type $\dot{\varepsilon} \propto \sigma^n$, a stress exponent of $n \sim 12$ resulted. All mechanical data at $\dot{\varepsilon} \sim 1 \times 10^{-5}\ s^{-1}$ are plotted as a function of reciprocal temperature in the Arrhenius graph of Fig. 3a. The one test performed at 770 °C showed anomalously high strength; the reason is unclear. Linear regression of the $1/T - \log\sigma$ data, excluding the 770 °C data point, illustrates the slightly higher strength of the dry samples compared with the wet samples. The slopes are not statistically different. Overall, the strengths of the marble samples used here are comparable with those observed previously for Carrara marble (Fig. 3b). At 1000 °C, however, the results of Schmid et al. (1980) fall significantly below those of the other studies.

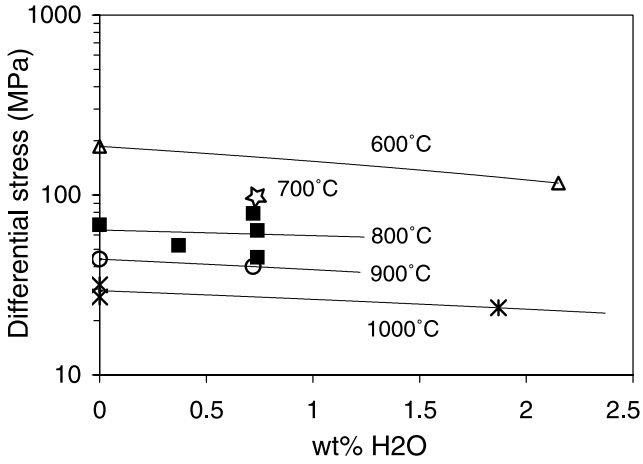

Fig. 2. Weight percentage water vs. differential stress measured at 5% axial strain. Trend lines are included to illustrate difference in strength between pre-dried and wet samples.

4. Microstructural observations

4.1. Starting material and heat-treated samples

The Carrara marble starting material (Fig. 4) consists of near-equidimensional grains (*Feret*90/*Feret*0 = 1.12 ± 0.02) with an arithmetic mean grain size of ~150 μm (Table 2). The grain size distribution is, in log-space, slightly negatively skewed (Fig. 4c). Grain boundaries are generally straight, with local fine-scale serrateness. However, grains are non-interlocking and can easily be separated. Grain boundaries often intersect at near-120° triple point junctions. Within individual grains, thin deformation (e-)twins with straight twin boundaries are present.

Microstructures of heat-treated dry and wet marble ($T=$ 800 °C) are shown in Fig. 5. Qualitatively, the microstructures are very similar to those of the starting material, but

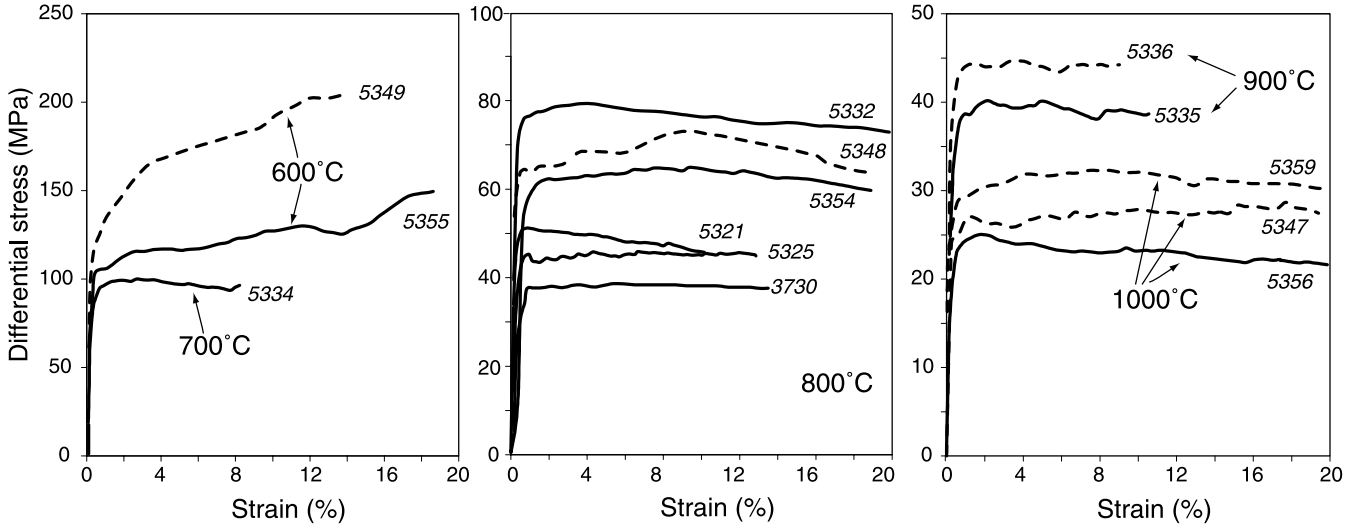

Fig. 1. Stress–strain curves for wet (continuous lines) and dried (dashed) Carrara marble deformed at $\dot{\varepsilon} \sim 1 \times 10^{-5}\ s^{-1}$ and various temperatures. Curves labeled with test no. (Table 2).

Table 2
Experimental details and microstructural data. *Samples 5321 and 5314 come from block Carr4, all others from Carr1 (see Table 1). T = temperature, $\dot{\varepsilon}$ = strain rate, ε = permanent axial strain at end of test, $\sigma(5\%)$ = flow (differential) stress at 5% strain, σ(end) = flow stress at end of test, s_1/s_3 is the strain ratio of ideal spherical grains deformed to shortening strain ε, N = number of grain measurements, d = grain size expressed as equivalent circular diameter (mean d refers to the arithmetic mean), P = grain perimeter, R = grain roundness (Eq. (1)), $F90/0 = Feret90/Feret0$ (grain aspect ratio measured perpendicular/parallel to load), F_s = grain aspect ratio normalized using s_1/s_3 (Eq. (2)), and D = grain perimeter/diameter fractal dimension (Eq. (3)). Standard deviation (sdev) and/or standard error of average values are included. **Pore fluid pressure constant (open system). All experiments carried out at confining pressure 300 MPa

Test#	Water [wt%]	T [°C]	$\dot{\varepsilon}$ [s^{-1}]	ε [%]	$\sigma(5\%)$ [MPa]	σ(end) [MPa]	s_1/s_3	N	Median d [μm]	Mean d [μm]	sdev	Error [μm]	P [μm]	Error [μm]	R	Error	$F90/0$	Error	F_s	Error	D	Error
Annealing tests:																						
Start	As is	–						220	137.0	147.5	74.2	5.0	559.5	18.8	1.41	0.02	1.12	0.02			0.957	0.010
5343	Dried	800						177	138.7	156.4	97.1	7.3	609.4	29.7	1.47	0.03	1.07	0.03			0.979	0.010
5331	1.80	800						217	135.0	148.4	79.6	5.4	557.3	20.0	1.39	0.02	1.04	0.02			0.955	0.008
Deformation tests:																						
5347	Dried	1000	1.4×10^{-5}	20.5	27.1	27.5	1.41	328	65.6	93.1	80.9	4.5	455.9	27.8	1.95	0.05	1.45	0.03	0.92	0.04	1.108	0.010
5359	Dried	1000	1.0×10^{-4}	21.0	31.7	30.3	1.42															
5356	1.87	1000	1.5×10^{-5}	21.0	23.6	21.6	1.42	727	40.3	63.6	61.6	2.3	300.4	12.3	1.88	0.03	1.26	0.02	0.79	0.03	1.093	0.006
5336	Dried	900	1.0×10^{-5}	8.5	44.0	44.2	1.14	247	92.9	120.6	92.2	5.9	565.9	34.4	1.92	0.05	1.23	0.03	0.97	0.04	1.067	0.012
5335	0.72	900	1.0×10^{-5}	9.4	40.0	38.7	1.16	229	110.8	133.2	99.0	6.5	570.8	29.1	1.79	0.04	1.37	0.04	1.06	0.05	1.006	0.009
5348	Dried	800	1.4×10^{-5}	19.7	68.3	63.9	1.39	788	51.3	66.7	53.7	1.9	329.2	11.0	2.14	0.03	1.54	0.02	0.99	0.03	1.112	0.008
5321*	0.37	800	1.0×10^{-5}	10.0	52.4	45.8	1.17															
5354	0.74	800	1.5×10^{-5}	18.1	63.4	59.7	1.35	603	54.2	75.1	65.4	2.7	366.7	15.5	2.10	0.04	1.38	0.02	0.92	0.03	1.078	0.008
5325	0.74	800	6.4×10^{-6}	12.6	45.1	44.5	1.22															
5332	0.72	800	1.0×10^{-5}	25.7	78.8	71.4	1.56															
3730	**	800	1.5×10^{-5}	13.4	38.3	37.6	1.24															
5314*	0.37	770	1.5×10^{-5}	9.5	114.4	110.2	1.16															
5334	0.74	700	1.0×10^{-5}	7.8	97.8	97.1	1.13	274	111.7	123.3	86.1	5.2	495.3	21.6	1.60	0.04	1.19	0.03	0.94	0.04	0.986	0.009
5349	Dried	600	1.4×10^{-5}	13.4	186.4	204.3	1.24	222	134.7	146.3	79.5	5.3	587.7	22.2	1.57	0.03	1.45	0.04	1.05	0.05	0.984	0.013
5355	2.15	600	1.7×10^{-5}	19.1	116.5	149.0	1.37	113	187.3	196.5	101.4	9.5	810.4	41.2	1.65	0.04	1.57	0.05	1.02	0.05	0.974	0.019

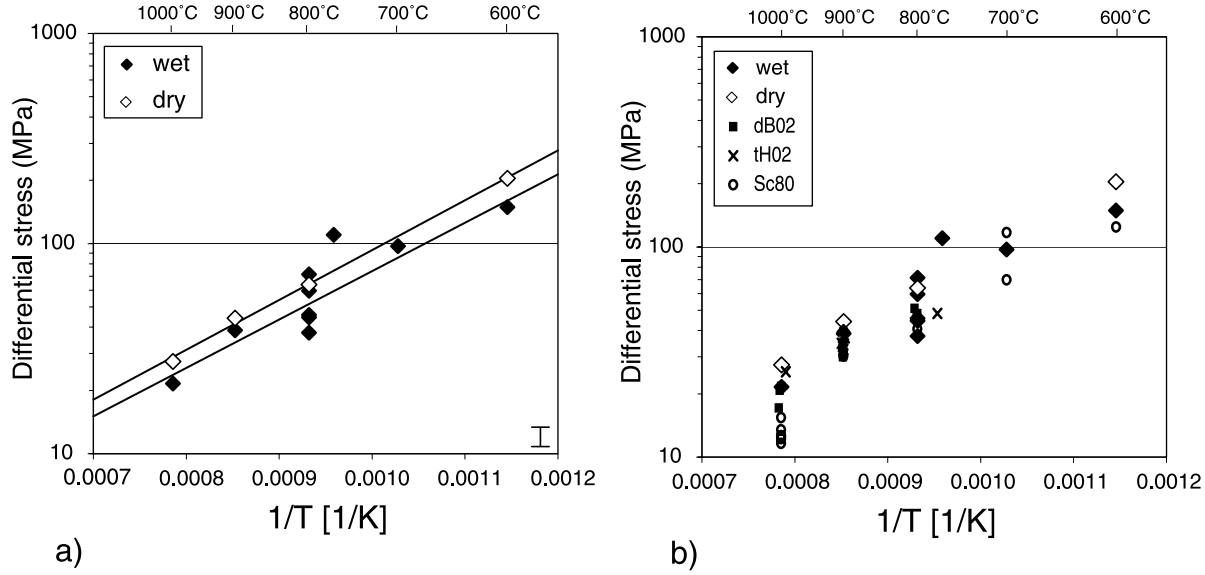

Fig. 3. Mechanical results of deformation experiments on wet and dry Carrara marble. (a) Differential stresses at $\dot{\varepsilon} \sim 1 \times 10^{-5}\ s^{-1}$ plotted against reciprocal temperature. Best fit lines are based on linear regression in $\log \sigma - 1/T$ space. The anomalous stress value at 770 °C (wet) was not included in the analysis. Note correspondence in slope between trends for wet and dry marble. Stress error bar given in lower right corner. (b) Stress–reciprocal temperature data at $\dot{\varepsilon} \sim 1 \times 10^{-5}\ s^{-1}$ from the present study and Schmid et al. (1980—Sc80), Ter Heege et al. (2002—tH02) and De Bresser (2002—dB02).

the small-scale irregularities seen in the grain boundaries of the starting material have largely disappeared (cf. Figs. 4b and 5b and e). In SEM, the heat-treated wet material shows pore structures with crystallographically controlled features (Fig. 5e). Measured grain size distributions (Fig. 5c and f) and average grain sizes (Table 2) are similar between starting material and heat-treated wet or dry marble. In contrast, the Feret ratio and average roundness of the calcite grains differ between samples; they are highest in the heat-treated dry sample and lowest in the heat-treated wet sample (Table 2).

4.2. Deformed samples

Light-optical microstructures and traced grain boundary maps of selected samples of dry- and wet-deformed marble are shown in Figs. 6 and 7, respectively. At 600 °C, both dry and wet samples show grain flattening, ubiquitous twinning and undulatory extinction in plane polarized light (Figs. 6a and b and 7a and b). Well-defined subgrains are virtually absent. No clear-cut evidence was found for dynamic recrystallization. At 800 °C, grain boundaries of original grains are serrated and subgrains are common (Figs. 6c and d and 7e and f). In addition, many small recrystallized grains (<30 μm diameter) are present. The larger grains contain only a few wide twins. No difference was immediately apparent between dry- and wet-deformed marble. At 900 °C, grain boundaries are lobate and 'orientation' families of grains showing the same interference color can be observed in polarized light, suggesting amoeboid grain shapes in 3D (Urai, 1983). Fewer subgrains and small recrystallized grains seem present compared with the samples deformed at 800 °C. Note, however, that the experiments at 900 °C did not reach the same strains as obtained at other temperatures (Table 2). Again, no qualitative difference was apparent between dry- and wet-deformed marble. Grain microstructures at 1000 °C are very irregular (Figs. 6e and f and 7i and j), with ubiquitous lobate grain boundaries, a large number of small recrystallized grains, and many orientation families. The wet-deformed samples appear to have more serrated, lobate grain boundaries than the dry samples, and fluid inclusion trails inside grain volumes are common. In all samples deformed at $T > 700$ °C, grain boundaries tend to show alignment in two conjugate directions at $\sim 45°$ to the compression direction ('diamond' shape structure; see Drury and Humphreys, 1988).

In SEM, split grain boundaries of dry samples are generally smooth with occasional pores (Fig. 8a–c). Grain boundaries of wet-deformed samples show an island structure of inclusion-free regions and isolated or locally semi-continuous remnants of fluid pockets (Fig. 8d–f). Pores locally show crystallographically controlled features. At 1000 °C, the pockets in grain boundaries of wet samples have irregular film-like morphologies (Fig. 8f).

Results of the microstructure quantification of the dry- and wet-deformed samples are included in Fig. 7 (grain size distributions) and Fig. 9 (average values for d, R and F_s). Note that dry and wet samples have been deformed to nominally the same axial strains at every individual temperature, so that measurements can be directly compared, but that final strains vary somewhat between temperatures (Table 2). For samples deformed at 600 °C, both the grain size distribution and the arithmetic mean

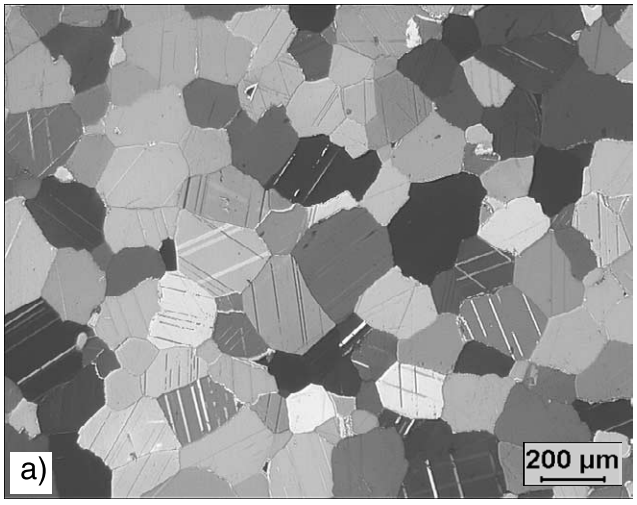

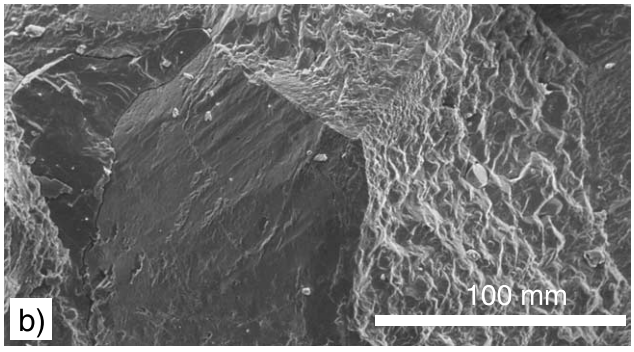

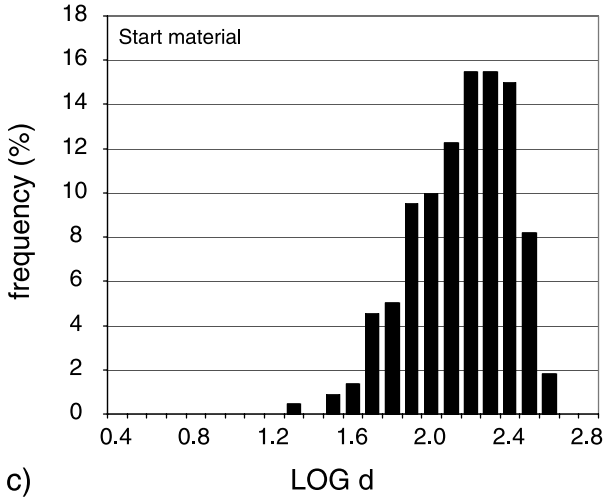

Fig. 4. Microstructures of Carrara marble starting material. (a) Transmitted light optical micrograph, plane polarized light, (b) SEM (secondary electron) image, (c) frequency histogram of grain size d (in µm).

grain size d of the dry material are very similar to those of the starting material (Figs. 7c and d and 9a). The distribution of the wet-deformed marble appears more irregular and the average d is larger. At 800 °C, the grain size distribution of the wet material shows a weak bimodal character that is absent in the dry sample (Fig. 7g and h). At 800 °C as well as 900 °C, the mean grain size of dry samples is slightly smaller than that of wet samples (Fig. 9a). In contrast, wet-deformed samples rather than dry samples have the smallest average grain size at 1000 °C (Fig. 9a). This is also apparent from the distribution histograms (Fig. 7k and l), where the grain size distribution of wet material at 1000 °C is positively skewed and shows a more pronounced peak at low d than does the distribution of dry marble at the same temperature. The data do not allow quantification of the percentage of recrystallized grains vs. old grains.

The value for the average grain roundness R of the deformed samples (Fig. 9b; Eq. (1)) is higher than that of the starting material at all temperatures investigated. At 600 °C, grains of the dry-deformed samples are slightly more circular than those of the wet samples (lower R value), at $T > 700$ °C the opposite was found. Grain aspect ratios normalized for the imposed strain, expressed as F_s (Eq. (2)), are shown in Fig. 9c. With increasing temperature, F_s progressively deviates from one, showing that the grain shape microstructure does not reflect total strain. This deviation is more pronounced in the wet samples (lower values for F_s), though the value at 900 °C is anomalously different.

Grain perimeters P and equivalent circular diameters d for two selected samples are plotted against each other in log-space in Fig. 10a. The data show a linear relationship that allows the fractal dimension D to be calculated, following (Takahashi et al., 1998):

$$P \propto d^D \tag{3}$$

Values for D have been determined for all individual samples of wet- and dry-deformed Carrara marble (Table 2), and are plotted against temperature in Fig. 10b. The values obtained for D for all wet samples consistently lie below those of dry-deformed samples. Further, a trend of increasing D with increasing temperature is apparent, though straightforward comparison of the data is hampered somewhat by the variation in final strain of samples deformed at different temperatures ($\varepsilon \approx 10\%$ at 700 and 900 °C, and $\varepsilon \approx 20\%$ at all other T; Fig. 10b).

5. Discussion

5.1. Summary of results and remarks on the efficiency of water infiltration

The results of this study suggest that water only mildly affects the high temperature mechanical behavior and microstructure development of Carrara marble Flow stresses of samples deformed in the presence of water are 10–40% lower than stresses of samples deformed dry at identical conditions, with one exception at 800 °C. Qualitatively, the microstructures of wet- and dry-deformed Carrara marble look very similar, but quantifiable grain parameters such as grain size, grain roundness and perimeter-diameter fractal dimension show small but

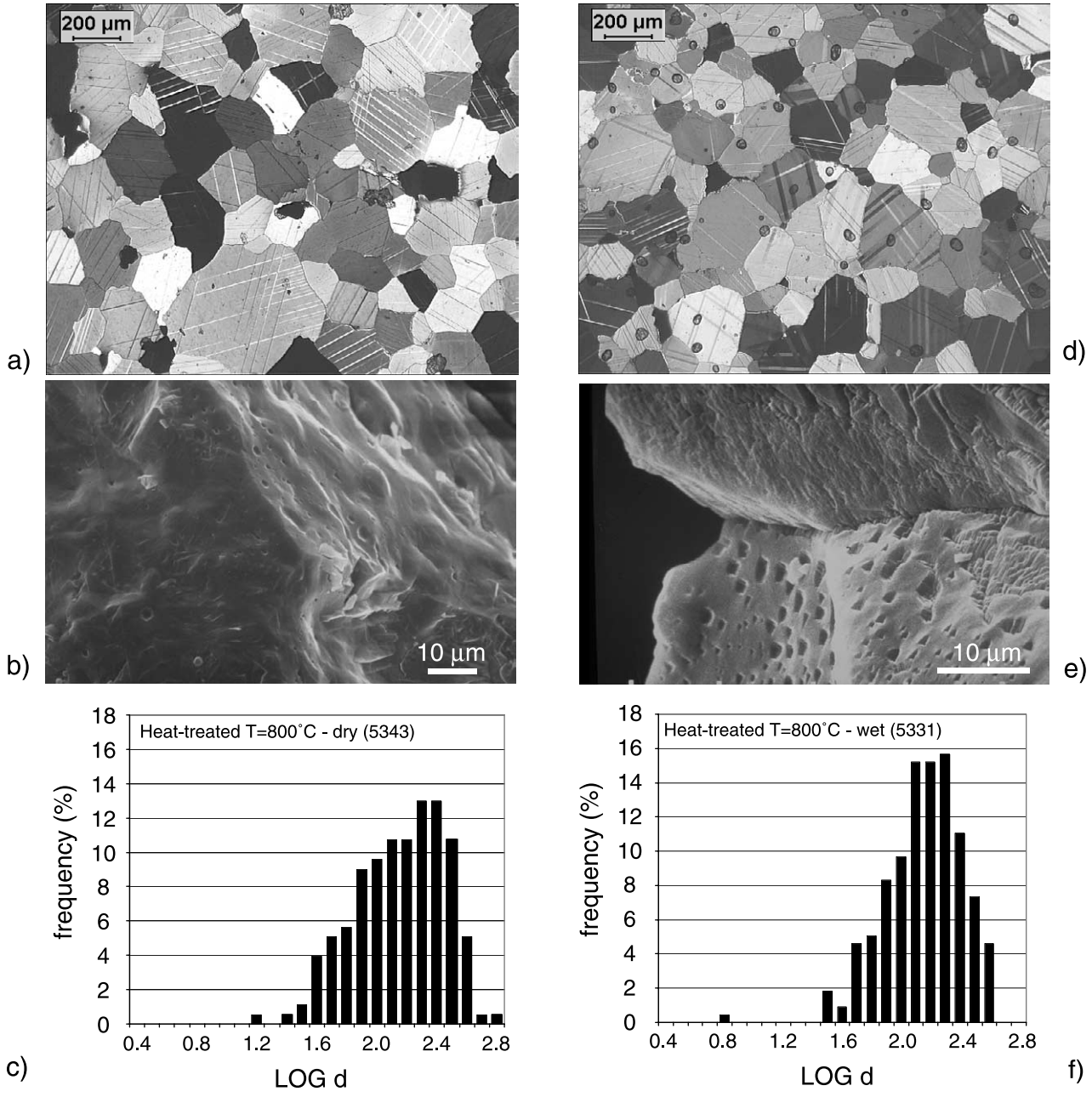

Fig. 5. Microstructures of Carrara marble heat-treated at 800 °C (see Table 2). (a) and (b) Light optical and SEM (secondary electron) image and (c) grain size distribution of heat-treated dry material (d in µm). (d)–(f) Idem for heat-treated wet marble. Note difference in SEM grain boundary structure (cf. Fig. 4b). Small bubbles visible in (d) are artifacts from thin section preparation.

statistically significant differences between wet and dry samples.

Two significant differences exist between the results for 600 °C and the results for 700–1000 °C: (1) stress–strain behavior at 600 °C showed continuous work hardening up to strains of ~20%, while near-steady state or strain weakening was observed at all higher temperatures (see Fig. 1), (2) the samples deformed at 600 °C did not show reduction in grain size, in spite of the relatively high flow stress, while all other samples ended up having a grain size that was smaller than that of the starting material (see Fig. 8). Because of these differences, the results at 600 °C need to be treated separately from the higher temperature results.

Before discussing the processes that might have caused the lower strength and different microstructures of wet Carrara marble compared with dry material, at 600 °C and at higher temperature, we have to ask the question if the water added to the samples effectively infiltrated the low porosity (~0.1%) marble. Rutter (1972, 1974) performed room temperature deformation experiments on dry and wet Carrara marble at different confining pressures, ranging from 0.1 to 300 MPa. He demonstrated that at high ratios (λ)

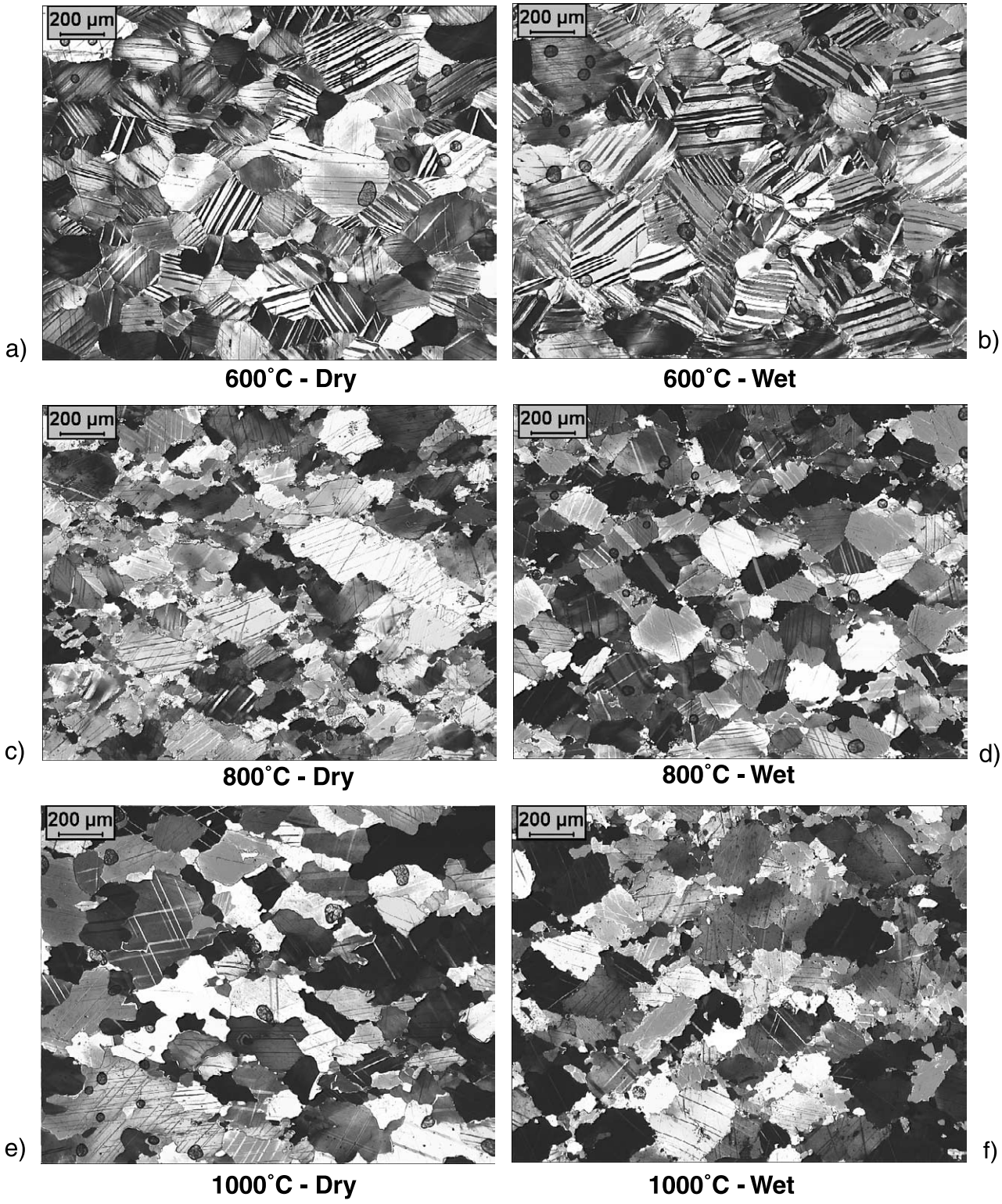

Fig. 6. Light optical microstructures of selected marble samples deformed with and without added water. All samples experienced axial strains of 18–21%, except for the sample deformed dry at 600 °C, for which $\varepsilon = 13\%$. Compression direction is vertical. Small bubbles visible are artifacts of thin section preparation.

of pore-fluid pressure to the total confining pressure the law of effective stress ('Terzaghi's law') holds for Carrara marble. This law describes the change in differential stress with increasing confining pressure at given λ. It followed that water must have been present along a significant fraction of the grain boundaries. Rutter (1974) also carried

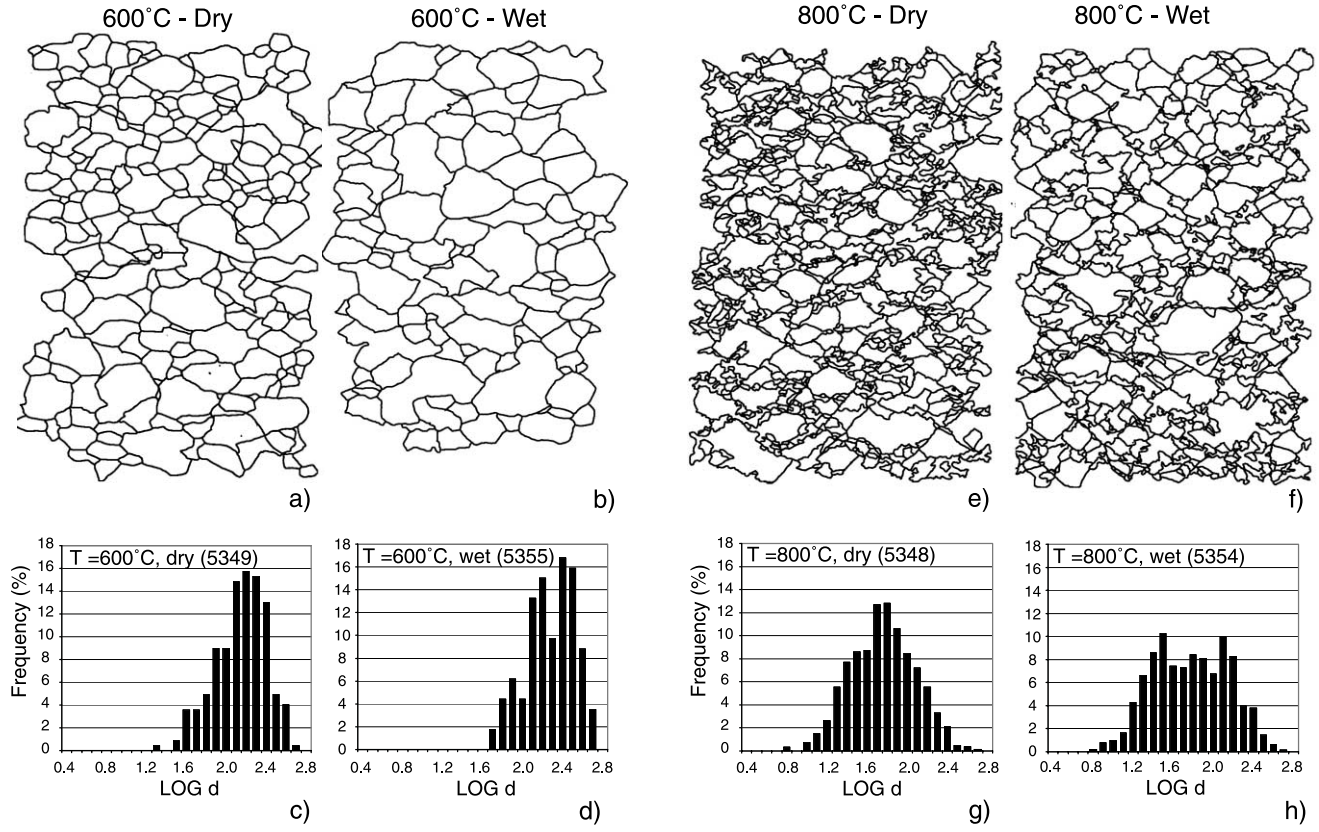
600˚C - Dry
600˚C - Wet
800˚C - Dry
800˚C - Wet
a)
b)
e)
f)
T =600˚C, dry (5349)
T =600˚C, wet (5355)
T =800˚C, dry (5348)
T =800˚C, wet (5354)
Frequency (%)
LOG d
c)
d)
g)
h)

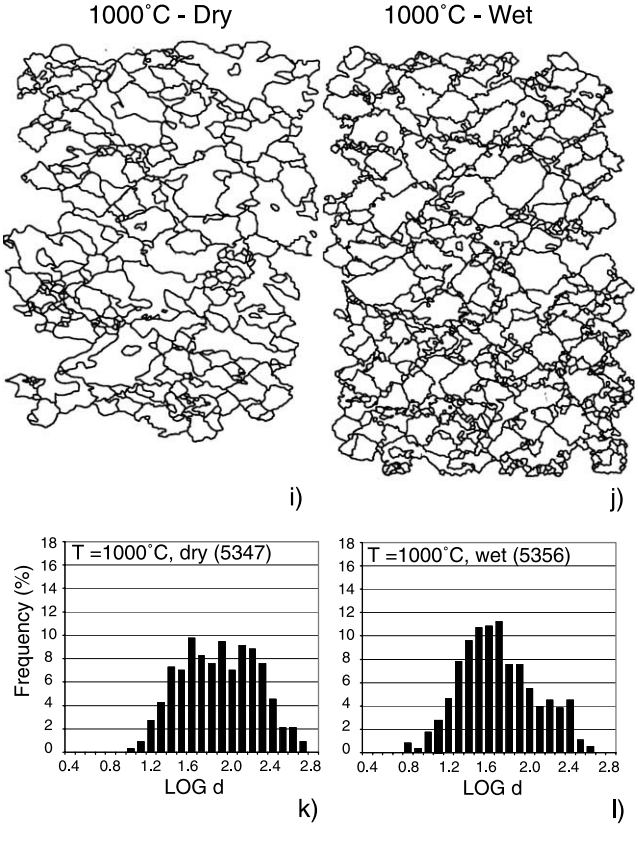
1000˚C - Dry
1000˚C - Wet
i)
j)
T =1000˚C, dry (5347)
T =1000˚C, wet (5356)
Frequency (%)
LOG d
k)
l)

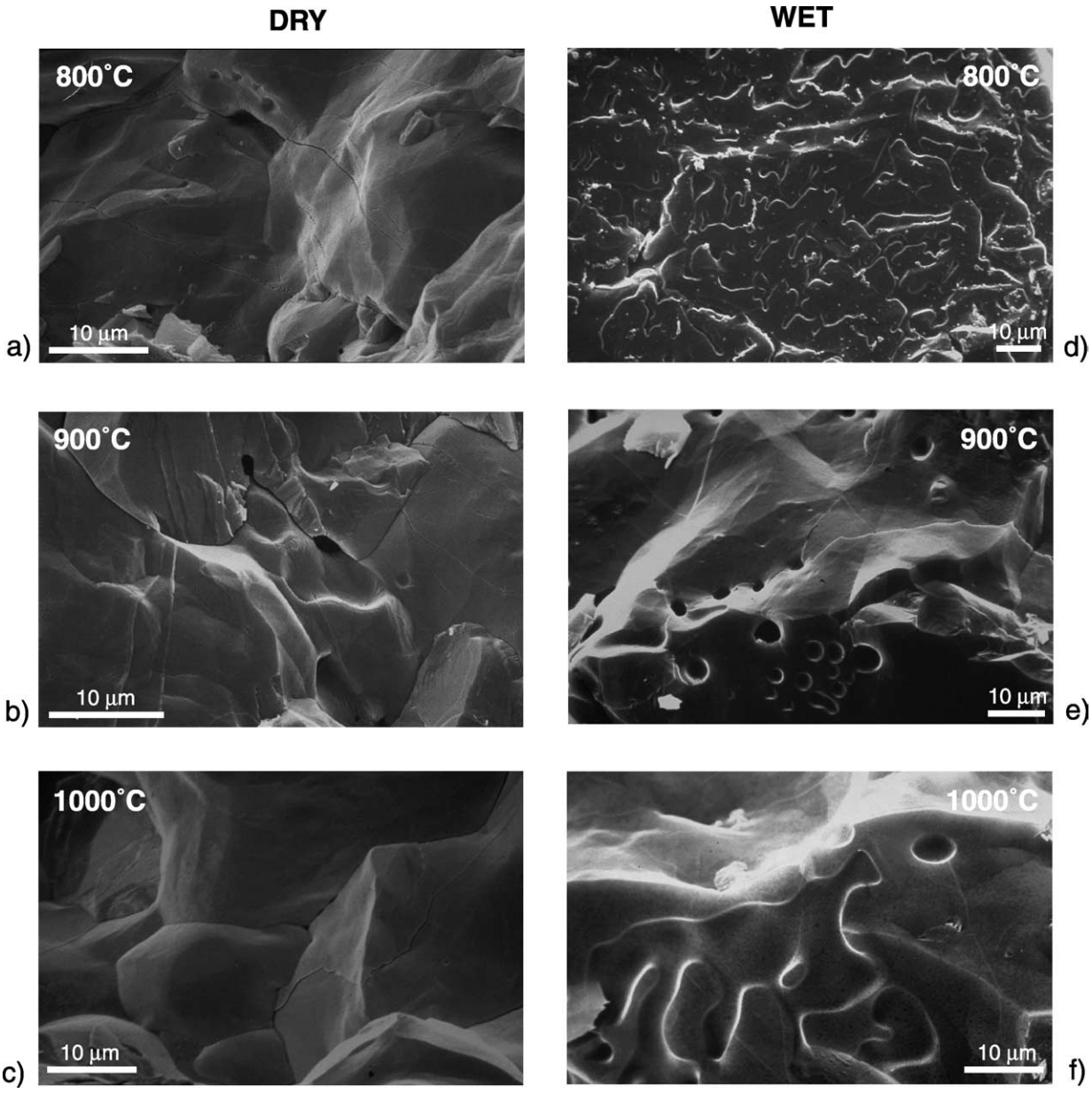

Fig. 8. SEM (secondary electron) images of dry and wet deformed Carrara marble. Wet samples generally show more pronounced island structures of inclusion free regions and isolated remnants of fluid pockets.

out one experiment at 400 °C in an experimental set-up equipped with a pore pressure system. In that test, water was pumped into the pores until the pore pressure was equal to the confining pressure. After the experiment, the sample could easily be disaggregated along the grain boundaries. This again is indicative that water infiltrated the grain boundaries. There is no reason to believe that our samples, all deformed at a confining pressure of 300 MPa, behaved any different from those of Rutter. The low initial porosity of our samples combined with the relatively high amounts of added water must have resulted in pore fluid pressures that were equal to the confining pressure, at least at the beginning of the experiments. This allowed samples to dilate and take up water. A rough estimation of the porosity created by the water phase, assuming that (a) all added water existed as pure H_2O fluid phase distributed through the sample and (b) pore fluid pressure was equal to confining pressure, resulted into values of 3–4% for most samples (0.7 wt% water—see Table 2), but varied from 2 to 10% depending on the amount of water added and deformation temperature.

Fig. 7. Traced grain boundary maps and grain size distribution histograms of same set of samples as illustrated in Fig. 6. Compression direction is vertical. d in μm.

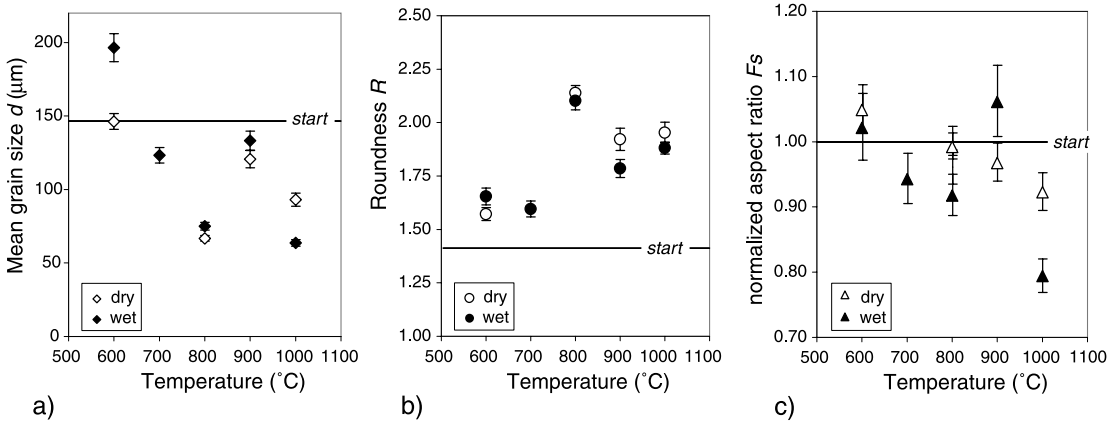

Fig. 9. Results of microstructure quantification using traced grain boundary maps (Fig. 7). Average values and standard errors as given in Table 2. (a) Arithmetic mean grain size d, (b) roundness R (Eq. (1)), (c) normalized grain aspect F_s (Eq. (2)); this ratio is an expression of the effectiveness of dynamic recrystallization in reworking the microstructure compared with the imposed flattening. 'Start' refers to values of starting material.

Further support for the interpretation that water infiltrated the grain boundaries of the Carrara marble comes from the difference in microstructure between wet- and dry-deformed samples seen in SEM (Fig. 7). Although pre-dried samples show occasional pores (see also Olgaard and Fitz Gerald, 1993), wet-deformed samples show substantially more pores.

The scatter in strength observed at 800 °C is larger than the variability normally observed between dry samples of Carrara marble coming from the same block (strengths reproducible within ~15%; see Schmid et al., 1980; Rutter, 1995; De Bresser, 2002; Ter Heege et al., 2002). Possibly the efficiency of fluid infiltration varied from one experiment to the next. We did not find any systematic relation between amount of water added and difference in strength (Table 2; Fig. 2).

5.2. Interpretation of the mechanical behavior in terms of deformation mechanisms

The observed mechanical behavior of Carrara marble, dry as well as wet, is very similar to that seen in previous studies on this material (Fig 3). At high temperature, deformation of Carrara marble is dominantly controlled by intracrystalline dislocation mechanisms (Schmid et al., 1980; De Bresser, 2002). The high value estimated for the apparent stress exponent for the present data ($n \sim 12$ at 1000 °C, cf. $n \sim 10$ in high strain torsion tests on Carrara marble at roughly the same temperature; Pieri et al., 2001) combined with the microstructural observations of grain flattening, undulatory extinction in plane polarized light, subgrain development and dynamic recrystallization confirm the importance of dislocation mechanisms.

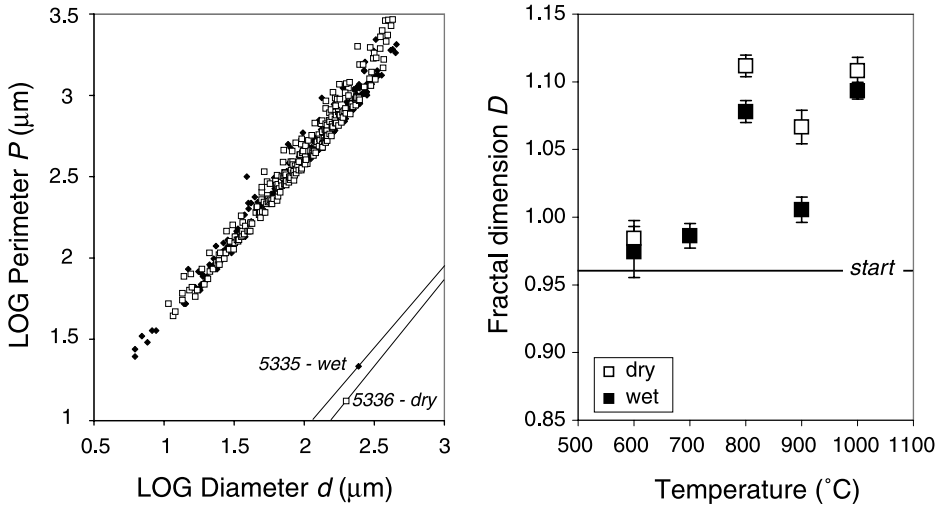

Fig. 10. Grain diameter/perimeter fractal dimension D (Eq. (3)) of deformed wet and dry samples (Table 2). (a) Grain diameters of two selected samples (T= 900 °C) vs. grain perimeters (see also Takahashi et al., 1998). Slopes of best fit lines given in lower right corner. (b) Fractal dimension D (Eq. (3)) of all samples vs. temperature. Note systematically lower value of D for wet samples compared with dry samples. 'Start' refers to D of starting material.

Nevertheless, the strength of wet marble was found to be slightly less than that of the dry material. What then is the cause of this weakening? We make the following points.

First, it is striking that the largest difference in strength between wet and dry Carrara marble developed at the lowest temperature tested (600 °C), where microstructure modification related to the presence of water was negligible. Fischer and Paterson (1992) determined permeability of Carrara marble at various (argon) pore fluid pressures and temperatures. They observed that if the temperature is raised to ~200 °C, the permeability is substantially enhanced due to dilatation associated with the anisotropy in thermal expansion of calcite. At $T>400$ °C, thermal recovery processes probably caused pore collapse and reversed this effect. We hypothesize that recovery processes are also responsible for the observed difference between our low temperature (600 °C) and higher temperature wet vs. dry experiments. At low temperature, high fluid pressure and dilatancy due to low effective pressure may have caused relatively high permeability and penetration of water into grain boundaries. This potentially induced a contribution of grain boundary sliding (GBS) to the overall creep rate of the wet material, causing weakening. Although active GBS might have resulted in a subsequent increase in pore space, reducing the pore fluid pressure and increasing the effective pressure, any ('dilatancy') hardening associated with this did not bring the strength of the wet marble to the level of the dry material. At temperatures above 600 °C, recovery mechanisms (dislocation climb or cross slip, dynamic recrystallization) became more prominent, allowing deformation to proceed at near steady state after some initial strain, but at the same time lowering the connectivity of the pores compared with lower temperatures (cf. Fischer and Paterson, 1992). As a consequence, the law of effective stress did not hold, and the effect of water in enhancing GBS was reduced. However, we do not imply that GBS was fully absent in the higher temperature tests. It is relevant in this respect to note that GBS has been observed to contribute to the creep of dry Carrara marble by Schmid et al. (1980) and Rutter (1995, his fig. 10), but only at $T\geqq700$ °C.

Second, no difference was observed between wet and dry data in terms of slopes of best-fit trends in $1/T-\log\sigma$ (Arrhenius) space (Fig. 3a), even excluding the data at 600 °, which still show hardening at the highest strains (Fig. 1). Since the trend in an Arrhenius plot is directly related to the microphysical mechanism(s) governing deformation (via the stress exponent n and activation energy Q if applying a standard Dorn-type creep law), we infer that the presence of water did not result in a major change in microphysical process(es) controlling the deformation. In other words, the dominant mechanism of dislocation recovery (climb, cross slip) that allowed deformation to proceed at quasi-steady state was the same in wet and dry Carrara marble. The slight differences in strength suggest that additional, second order mechanisms were involved in the deformation of marble at high temperature (e.g. combined dislocation and diffusion and/or GBS processes; see Pieri et al., 2001; Ter Heege et al., 2002), and that small shifts in relative importance of the contributing mechanisms resulted depending on the presence or absence of water.

Third, as an alternative to the possible role of water in enhancing GBS and/or affecting the type of dislocation recovery mechanism, the lower strength of the wet samples could be attributed to a difference in geometrical configuration of dislocations in the deforming grains and a related change in rate (but not mechanism) of recovery. This would affect the pre-exponential constant in a creep law. In this, water fugacity might play a role (e.g. Kohlstedt et al., 1995; Rybacki and Dresen, 2000), but the present data do not allow assessment of this effect.

Thus the mechanical data alone are insufficient to conclude what the influence of water was on the deformation mechanism governing high temperature creep of marble. However, a clear correlation was found between the small variation in strength and the subtle differences in grain microstructure between dry and wet marble, notably at the higher temperatures (Figs. 9 and 10). Therefore, water may have influenced the process of dynamic recrystallization, in particular the migration of grain boundaries, and in turn recrystallization may have affected the strength.

5.3. Grain boundary mobility in dry and wet marble at $T=600$ °C

At 600 °C, there is little evidence of significant dynamic recrystallization in either wet- or dry-deformed marble. Further, the mean grain size d of the dry-deformed sample is almost the same as d of the starting material (some apparent grain size reduction can be expected due to the non-plane strain geometry of the deformation experiments; see Section 2). The wet sample, however, shows a somewhat different grain size distribution (Fig. 7c and d) and substantially larger mean grain size (Fig. 9a). From the heat treatment tests at higher temperature ($T=800$ °C) it is known that virtually no static grain growth takes place over the time of the experiment (Table 2). Consequently, the larger grain size in the wet sample must be the result of either water-enhanced dynamic (i.e. stress-induced) grain growth or a different initial value of the grain size (i.e. some inhomogeneity of the original block of white marble). The latter option seems more probable since twin-microstructures of the wet sample (Fig. 6b) give no indication of enhanced grain boundary mobility compared with the dry sample, evidenced for example by twins that abruptly end within the volume of a grain, effectively being left behind after grain boundary migration. Further, the average grain aspect ratio (*Feret*90/*Feret*0, Table 2) of the sample lies close to the value expected on the basis of strain alone ($F_s\approx1$, Fig. 8c), while this is unlikely to be the case if substantial grain growth had occurred.

5.4. Grain boundary mobility in dry and wet marble at T= 700–1000 °C

Dynamic recrystallization reduced the grain size of the samples deformed at 700–1000 °C With one exception (900 °C), the grain aspect ratios of the deformed samples are lower than expected based on the amount of strain. With increasing temperature, the deviation between measured grain aspect ratio and strain ratio, F_s (Fig. 9c), becomes more pronounced (values progressively deviating from one), both for dry and wet samples. This decrease in F_s illustrates the increased effectiveness of dynamic recrystallization towards higher temperature. Moreover, the values for F_s of wet samples are generally smaller than of dry, suggesting that the grain boundary mobility of wet samples was higher than of dry samples. We conclude that these measurements form a quantitative illustration of some fluid-enhanced migration recrystallization (e.g. Urai, 1983, 1985; Drury and Urai, 1990). It is unclear why the data point for wet Carrara marble at 900 °C is an outlier, but this might be related to the lower strain in this test compared with the others.

Olgaard and Evans (1988) investigated static grain growth in synthetic marbles with water and different amounts of pores and mica. Minor amounts of pores or mica particles inhibited normal grain growth by pinning grain boundaries. If pores were water-filled, grain growth was hindered but not arrested. Covey-Crump (1997) demonstrated that under dry conditions grain boundary mobility in synthetic calcite aggregates is very sensitive to trace solute impurity concentrations. In the presence of pore fluids, grain growth was enhanced and less sensitive to calcite purity. Grain boundary migration is also promoted if new driving forces, such as from strain energy, are introduced that allow unpinning of boundaries or dragging of pores or inclusions. The pervasive microstructural modification of all Carrara marble samples deformed at T>600 °C shows that these dynamic forces were indeed produced during deformation, in both wet and dry material. Grain boundary mobility was enhanced by the presence of water, and was associated with a small decrease in strength.

The precise mechanism by which grain boundary migration reduced the strength of the marble remains unknown, but several possibilities can be put forward. First, the enhanced grain boundary migration rate in wet samples might have resulted in a more efficient removal of 'hard' grains and development of new grains with little substructure and/or easy slip orientation (e.g. Poirier, 1980; see also Pieri et al., 2001). Second, fluid-assisted grain boundary migration could point to solution–precipitation processes contributing to the overall creep and weakening of the material, as suggested for carnallite (Urai, 1985) and halite (Ter Heege, 2002; Watanabe and Peach, 2002). This might not seem probable in the case of calcite given its low solubility in pure water at low temperature and pressure, and the even further decrease in solubility if temperature is raised, but recent experiments by Caciagli and Manning (2003) have shown that at high temperature and pressure (T=500–800 °C, pressure ≧300 MPa) calcite becomes more soluble again (but see Section 5.5 on partial melting at high T). A third possibility, already touched upon in Section 5.2, is suggested by our measurements of grain roundness R and fractal dimension D. Values for R and D for wet deformed and recrystallized samples (T>600 °C; Figs. 9c and 10b) are systematically lower than for dry samples, implying that, on average, grains in wet samples have less irregular, more rounded shapes. It is recalled that Schmid et al. (1980) and Rutter (1995) found microstructural evidence for active GBS in dry Carrara marble at T≧700 °C, contributing up to half of the overall strain in certain samples. The grain boundary (diamond shape) alignment in the present samples (Fig. 6c–f) forms further support for GBS, in interaction with grain boundary migration (Urai et al., 1986b; Drury and Humphreys, 1988). Adding water could have promoted the development of a grain shape that made the wet marble more prone to GBS processes. It was argued above that enhanced GBS might be the reason for the rather large difference in strength between wet and dry (non-recrystallized) marble at 600 °C, but that this effect can be expected to be less at higher temperature due to more efficient recovery processes (cf. Fischer and Paterson, 1992) and associated redistribution of water into unconnected pockets (cf. Fig. 8). The observed small difference in strength (∼10%) between dry and wet marble at high temperature is consistent with this.

5.5. Partial melting

In the discussion above we argued that water helped migration recrystallization by enhancing grain boundary mobility However, water also lowers the melting point of calcite (Wyllie and Boettcher, 1969). Olgaard (1985) and Olgaard and Evans (1988) found thin intergranular films of amorphous or crypto-crystalline material in wet samples of fine-grained calcite rock at 700 °C, and they interpreted this as evidence for partial melting. Also Rutter (1984) reported microstructural evidence for melting in grain boundaries at T≧700 °C, in samples of fine-grained Solnhofen limestone (d=5 μm) tested for grain growth under the presence of water. Grain size measurements by Rutter demonstrated limited initial coarsening followed by grain size stabilization in dry samples, while samples with grain boundary melt showed ongoing grain growth. This was interpreted as indicating that grain coarsening is suppressed in dry samples by the presence of small amounts of impurities in the grain boundaries (see also Berger and Herwegh (2004), for natural carbonate rocks), but that these impurities dissolved in the melt that developed in water-added samples, resulting in removal of the inhibition of growth. Experiments by Renner et al. (2002a) confirmed the direct relation between grain boundary mobility in calcite aggregates and the diffusion kinetics of secondary phases on grain boundaries. Boundary mobility was very low in samples with solid secondary

phases or pores filled with inert gas (effective pinning), but increased if pores were filled with hydrous phases or, even more, with melt (pores could be left behind or dragged along with migrating grain boundaries).

Given the deformation conditions applied to our samples, some partial melting of the marble is likely to have taken place at the higher temperatures investigated. Accordingly, some of the remnants of fluid pockets seen in the samples (e.g. Fig. 8e) can be interpreted as quenched melts. The difference in strength between wet and dry Carrara marble deformed at $T > 700$ °C might thus only be indirectly related to water content. Water may have promoted the development of melt that in turn enhanced the grain boundary mobility (cf. Rutter, 1984; Renner et al., 2002a). This resulted in recrystallization microstructures that were slightly different from those of dry-deformed Carrara marble, affecting the mechanical behavior of the material (i.e. via enhanced contribution of GBS).

5.6. Quantitative constraints on microstructure modification of wet vs dry deformed marble

In general, the observed microstructures of our deformed marbles are very similar to the structures described in earlier studies of Carrara marble (Schmid et al., 1980; Rutter, 1995; Ter Heege et al., 2002). Differences between wet and dry material only become apparent when microstructural parameters such as grain roundness and grain diameter/perimeter fractal dimension are quantified. The absolute values for these parameters cannot be used as indicators for deformation under wet or dry conditions, since temperature and strain are also of influence. This is best illustrated by looking at the values for the fractal dimension D (Fig. 10). At all temperatures investigated, D for dry samples is higher than for wet samples, but the value for D for dry marble at 900 °C is *lower* than that for wet marble at 800 °C as well as 1000 °C. We suggest that D can be used as an indicator for deformation under dry or wet conditions if marbles from the same geological setting are studied, so that similar deformation temperature and strain can be assumed.

Kruhl and Nega (1996) analyzed quartz grains in various igneous and metamorphic rocks, and suggested that the grain diameter/perimeter fractal dimension D can be used as a temperature indicator. With increasing temperature, the values for D decreased. Takahashi et al. (1998) found similar results in experimentally deformed quartzites. The latter authors extend the application of D by suggesting that it can also be used as a strain rate indicator; D increases with increasing strain rate. The present results on Carrara marble are not consistent with the results on deformed quartzite: (a) with increasing temperature at constant strain rate, D of Carrara marble increases rather than decreases, and (b) a difference between wet and dry samples emerged, while water was not taken into account in a systematic way in the previous studies concerning D. Consequently, one has to be cautious in interpreting values of D as direct indicators of deformation conditions.

6. Summary and conclusions

We have performed axial compression tests on wet (0.4–2.1 wt% water) and pre-dried samples of Carrara marble. Deformation conditions were $T = 600$–1000 °C, confining pressure 300 MPa and strain rate $\dot{\varepsilon} \sim 1 \times 10^{-5}\ s^{-1}$, with one test carried out at $\dot{\varepsilon} \sim 1 \times 10^{-4}\ s^{-1}$. Our aim was to investigate the effect of water on microstructure modification of marble in relation to the mechanical behavior. We conclude the following:

1. Adding distilled water to Carrara marble has only a small effect on the mechanical behavior and development of microstructure at high temperature.
2. At laboratory strain rate and $T = 600$ °C dynamic recrystallization is unimportant, but wet marble may be up to 40% weaker than pre-dried samples of the same material. We suggest that this strength difference is caused by high pore fluid pressure enhancing dilatation and assisting contribution of grain boundary sliding (GBS) to creep.
3. At laboratory strain rate and $T \geqq 700$ °C, dynamic recrystallization is more prominent than at lower temperatures, resulting in substantial reworking of the microstructure. Subtle differences exist between wet and dry marble, expressed using microstructure parameters such as grain size, grain roundness and perimeter-area fractal dimension. However, the difference in strength between wet and dry marble is less than at lower temperature, not exceeding, on average, 10%. Apparently, dynamic recrystallization acts as a recovery process that reduces (but not necessarily prevents) the contribution of GBS to creep.
4. Quantification of grain microstructures indicates slightly higher grain boundary mobility in wet samples than in dry material, implying that fluid-enhanced grain boundary migration recrystallization was active in the marble. At the highest temperatures investigated, the effect of water might have been indirect, by producing small amounts of melt that affected grain boundary mobility. As a result of the enhanced grain boundary mobility in wet samples, less irregular grain shapes developed compared with dry marble, potentially making GBS slightly easier. Earlier work on Carrara marble demonstrated GBS to take place at high temperature; our results suggest that water, directly or indirectly, enhances this mechanism.
5. Values for parameters describing microstructural features can help distinguish wet from dry deformed marble. In particular, the grain diameter/perimeter fractal dimension D of wet recrystallized marble is consistently smaller than that of dry marble.

Water is well known to cause substantial rheological weakening of Earth materials such as quartz, olivine and halite. In contrast, the effect of water on the strength of calcite marble at high temperature is small. Consequently, there appears little reason to take this parameter into account when analyzing weakening and associated strain localization in coarse-grained calcite rocks.

Acknowledgements

Frank Strozyk (RWTH-Aachen) is thanked for arduously mapping the microstructures of the deformed Carrara marble. We also thank Oliver Schenk for discussing microstructures of wet and dry natural marbles and for carefully reading an early version of the manuscript. At ANU (Canberra), Stephen Cox, Jan Bitmead and Graeme Horwood helped with the experiments, John Fitz Gerald assisted with SEM, and Mervyn Paterson contributed by numerous discussions. G. Molli and E. Rutter are thanked for reviews that improved the manuscript.

References

Adams, F.D., Nicolson, J.T., 1900. An experimental investigation into the flow of marble. Philosophical Transactions of the Royal Society of London, Series A 195, 363–401.

Berger, A., Herwegh, M., 2004. Grain coarsening in contact metamorphic carbonates: effects of second-phase particles, fluid flow and thermal perturbations. Journal of Metamorphic Geology 22, 459–474.

Caciagli, N.C., Manning, C.E., 2003. The solubility of calcite in water at 6–16 kbar and 500–800 °C. Contributions to Mineralogy and Petrology 146, 275–285.

Carter, N.L., Kronenberg, A.K., Ross, J.V., Wiltschko, D.V., 1990. Control of fluids on deformation of rocks, in: Knipe, R.J., Rutter, E.H. (Eds.), Deformation Mechanism, Rheology and Tectonics Geological Society, London, Special Publications, 54, pp. 1–13.

Covey-Crump, S.J., 1997. The normal grain growth behaviour of nominally pure calcitic aggregates. Contributions to Mineralogy and Petrology 129, 239–254.

De Bresser, J.H.P., 2002. On the mechanism of dislocation creep of calcite at high temperature: inferences from experimentally measured pressure sensitivity and strain rate sensitivity of flow stress. Journal of Geophysical Research 107, B12, 2337, DOI: 10.1029/2002JB001812.

De Bresser, J.H.P., Evans, B., Renner, J., 2002. On estimating the strength of calcite rocks under natural conditions, in: De Meer, S., Drury, M.R., De Bresser, J.H.P., Pennock, G.M. (Eds.), Deformation Mechanisms, Rheology and Tectonics: Current Status and Future Perspectives Geological Society, London, Special Publications, 200, pp. 309–332.

De Meer, S., Drury, M.R., De Bresser, J.H.P., Pennock, G.M., 2002. Current issues and new developments in deformation mechanisms, rheology and tectonics, in: De Meer, S., Drury, M.R., De Bresser, J.H.P., Pennock, G.M. (Eds.), Deformation Mechanisms, Rheology and Tectonics: Current Status and Future Perspectives Geological Society, London, Special Publications, 200, pp. 1–27.

Dewers, T., Muhuri, S., 2000. Transition from plastic to viscous flow in aggregate granular creep. EOS, Transactions, American Geophysical Union 81, F1187.

Drury, M.R., Humphreys, F.J., 1988. Microstructural shear criteria associated with grain-boundary sliding during ductile deformation. Journal of Structural Geology 10, 83–89.

Drury, M.R., Urai, J.L., 1990. Deformation-related recrystallization processes. Tectonophysics 172, 235–253.

Fischer, G.J., Paterson, M.S., 1992. Measurement of permeability and storage capacity in rocks during deformation at high temperature and pressure, in: Evans, B., Wong, T-f. (Eds.), Fault Mechanics and Transport Properties of Rocks. Academic Press, London, pp. 213–252.

Griggs, D.T., Turner, F.J., Borg, I., Sosoka, J., 1951. Deformation of Yule marble, Part IV. Bulletin of the Geological Society of America 62, 1385–1406.

Griggs, D.T., Turner, F.J., Borg, I., Sosoka, J., 1953. Deformation of Yule marble, Part V—effects at 300 °C. Bulletin of the Geological Society of America 64, 1327–1342.

Heard, H.C., 1960. Transition from brittle fracture to ductile flow in Solenhofen limestone as a function of temperature, confining pressure, and interstitial fluid pressure. The Geological Society of America, Memoir 79, 193–226.

Heilbronner, R., Tullis, J., 2002. The effect of static annealing on microstructures and crystallographic preferred orientations of quartzites experimentally deformed in axial compression and shear, in: De Meer, S., Drury, M.R., De Bresser, J.H.P., Pennock, G.M. (Eds.), Deformation Mechanisms, Rheology and Tectonics: Current Status and Future Perspectives Geological Society, London, Special Publications, 200, pp. 191–218.

Hirth, G., Kohlstedt, D.L., 1995. Experimental constraints on the dynamics of the partially molten upper mantle: deformation in the diffusion creep regime. Journal of Geophysical Research 100, 1981–2001.

Hirth, G., Kohlstedt, D.L., 1996. Water in the oceanic upper mantle: implications for rheology, melt extraction and the evolution of the lithosphere. Earth and Planetary Science Letters 144, 93–108.

Jung, H., Karato, S-i., 2001. Water-induced fabric transitions in olivine. Science 239, 1460–1463.

Karato, S-i., Paterson, M.S., Fitz Gerald, J.D., 1986. Rheology of synthetic olivine aggregates: influence of grain size and water. Journal of Geophysical Research 91, 8151–8176.

Kohlstedt, D.L., Evans, B., Mackwell, S.J., 1995. Strength of the lithosphere: constraints imposed by laboratory experiments. Journal of Geophysical Research 100, 17587–17602.

Kronenberg, A.K., Kirby, S.H., Aines, R.D., Rossman, G.R., 1986. Solubility and diffusional uptake of hydrogen in quartz at high water pressure: implications for hydrolytic weakening. Journal of Geophysical Research 91, 12723–12744.

Kronenberg, A.K., Segall, P., Wolf, G.H., 1990. Hydrolytic weakening and penetrative deformation within a natural shear zone, in: Duba, A.G., Durham, W.B., Handin, J.W., Wang, H.F. (Eds.), The Brittle–Ductile Transition in Rocks (The Heard Volume) Geophysical Monograph, 56. American Geophysical Union, Washington, DC, pp. 21–36.

Kruhl, J.H., Nega, M., 1996. The fractal shape of sutured quartz grain boundaries: application as a geothermometer. Geologische Rundschau 85, 38–43.

McDonnell, R.D., Peach, C.J., Spiers, C.J., 1999. Flow behavior of fine-grained synthetic dunite in the presence of 0.5 wt% H_2O. Journal of Geophysical Research 104, 17823–17845.

Mei, S., Kohlstedt, D.L., 2000a. Influence of water on plastic deformation of olivine aggregates 1. Diffusion creep regime. Journal of Geophysical Research 105, 21457–21469.

Mei, S., Kohlstedt, D.L., 2000b. Influence of water on plastic deformation of olivine aggregates 2. Dislocation creep regime. Journal of Geophysical Research 105, 21471–21481.

Olgaard, D.L., 1985. Grain growth and mechanical processes in two-phased synthetic marbles and natural fault gouge. PhD thesis, Massachusetts Institute of Technology, Cambridge, Massachusetts, 204pp.

Olgaard, D.L., Evans, B., 1988. Grain growth in synthetic marbles with added mica and water. Contributions to Mineralogy and Petrology 100, 246–260.

Olgaard, D.L., Fitz Gerald, J.D., 1993. Evolution of pore microstructures during healing of grain boundaries in synthetic calcite rocks. Contributions to Mineralogy and Petrology 115, 138–154.

Paterson, M.S., 1990. Rock deformation experimentation, in: Duba, A.G., Durham, W.B., Handin, J.W., Wang, H.F. (Eds.), The Brittle–Ductile Transition in Rocks (The Heard Volume) Geophysical Monograph, 56. American Geophysical Union, Washington, DC, pp. 187–194.

Peach, C.J., Spiers, C.J., Trimby, P.W., 2001. Effect of confining pressure on dilatation, recrystallization, and flow of rock salt at 150 °C. Journal of Geophysical Research 106, 13315–13328.

Pieri, M., Burlini, L., Kunze, K., Stretton, I., Olgaard, D.L., 2001. Rheological and micro structural evolution of Carrara Marble with high shear strain; results from high temperature torsion experiments. Journal of Structural Geology 23, 1393–1413.

Poirier, J.P., 1980. Shear localization and shear instability in materials in the ductile field. Journal of Structural Geology 2, 135–142.

Post, A.D., Tullis, J., Yund, R.A., 1996. Effects of chemical environment on dislocation creep of quartzite. Journal of Geophysical Research 101, 22143–22155.

Renner, J., Evans, B., Hirth, G., 2002a. Grain growth and inclusion formation in partially molten carbonate rocks. Contributions to Mineralogy and Petrology 142, 501–514.

Renner, J., Evans, B., Siddiqi, G., 2002b. Dislocation creep of calcite. Journal of Geophysical Research 107, B12, 2364, DOI: 10.1029/2001B001680.

Rubie, D.C., 1990. Mechanisms of reaction-enhanced deformability in minerals and rocks, in: Barber, D.J., Meredith, P.G. (Eds.), Deformation Processes in Minerals, Ceramics and Rocks. Unwin Hyman, London, pp. 262–295.

Rutter, E.H., 1972. The influence of interstitial water on the rheological behaviour of calcite rocks. Tectonophysics 14, 13–33.

Rutter, E.H., 1974. The influence of temperature, strain rate and interstitial water in the experimental deformation of calcite rocks. Tectonophysics 22, 311–334.

Rutter, E.H., 1984. The kinetics of grain coarsening in calcite rocks. Progress in Experimental Petrology (NERC) 6, 245–249.

Rutter, E.H., 1995. Experimental study on the influence of stress, temperature and strain on the dynamic recrystallization of Carrara marble. Journal of Geophysical Research 100, 24651–24663.

Rutter, E.H., Brodie, K.H., 1995. Mechanistic interactions between deformation and metamorphism. Geological Journal 30, 227–240.

Rybacki, E., Dresen, G., 2000. Dislocation and diffusion creep of synthetic anorthite aggregates. Journal of Geophysical Research 105, 26017–26036.

Schmid, S.M., Paterson, M.S., Boland, J.N., 1980. High temperature flow and dynamic recrystallization in Carrara marble. Tectonophysics 65, 245–280.

Spiers, C.J., Carter, N.L., 1998. Microphysics of rocksalt flow in nature, in: Aubertin, M., Hardy, H.R. (Eds.), The Mechanical Behavior of Salt Proceedings of the 4th Conference, Trans. Tech. Publ. Series on Rock and Soil Mechanics, 22, pp. 115–128.

Takahashi, M., Nagahama, H., Masuda, T., Fujimura, A., 1998. Fractal analysis of experimentally, dynamically recrystallized quartz grains and its possible application as a strain rate meter. Journal of Structural Geology 20, 269–275.

Ter Heege, J.H., 2002. Relationship between dynamic recrystallization, grain size distribution and rheology. Geological Ultraiectina 218, PhD thesis, Utrecht University, The Netherlands, 141pp.

Ter Heege, J.H., De Bresser, J.H.P., Spiers, C.J., 2002. The influence of dynamic recrystallization on the grain size distribution and rheological behaviour of Carrara marble deformed in axial compression, in: De Meer, S., Drury, M.R., De Bresser, J.H.P., Pennock, G.M. (Eds.), Deformation Mechanisms, Rheology and Tectonics: Current Status and Future Perspectives Geological Society, London, Special Publications, 200, pp. 331–353.

Tullis, J., Yund, R.A., 1991. Experimental evidence for diffusion creep in feldspar aggregates. Journal of Structural Geology 13, 987–1000.

Urai, J.L., 1983. Water assisted dynamic recrystallization and weakening in polycrystalline bischofite. Tectonophysics 96, 125–157.

Urai, J.L., 1985. Water assisted dynamic recrystallization and solution transfer in experimentally deformed carnallite. Tectonophysics 120, 285–317.

Urai, J.L., Means, W.D., Lister, G.S., 1986a. Dynamic recrystallization of minerals, in: Hobbs, B.E., Heard, H.C. (Eds.), Mineral and Rock Deformation: Laboratory Studies (The Paterson Volume) Geophysical Monograph, 36. American Geophysical Union, Washington, DC, pp. 161–200.

Urai, J.L., Spiers, C.J., Zwart, H.J., Lister, G.S., 1986b. Weakening of rocksalt by water during long term creep. Nature 324, 554–557.

Van der Molen, I., Paterson, M.S., 1979. Experimental deformation of partially-melted granite. Contributions to Mineralogy and Petrology 70, 299–318.

Watanabe, T., Peach, C.J., 2002. Electrical impedance measurement of plastically deforming halite rocks at 125 °C and 50 MPa. Journal of Geophysical Research 107, B1, 2004, DOI: 10.1029/2001B000204.

Wyllie, P.J., Boettcher, A.L., 1969. Liquidus phase relationships in the system $CaO–CO_2–H_2O$ to 40 kilobars pressure with petrological applications. American Journal of Science 267A 1969;, 489–508.

Zhang, X., Salemans, J., Peach, C.J., Spiers, C.J., 2002. Compaction experiments on wet calcite powder at room temperature: evidence for the operation of intergranular pressure solution, in: De Meer, S., Drury, M.R., De Bresser, J.H.P., Pennock, G.M. (Eds.), Deformation Mechanisms, Rheology and Tectonics: Current Status and Future Perspectives Geological Society, London, Special Publications, 200, pp. 29–39.